JTEIN: Jurnal Teknik Elektro Indonesia, Vol. 7, No. 1, pp. 35-44, 2026
e-ISSN 2723-0589

Two-Layer Fractional Frequency Reuse With Bandwidth Partitioning for 3.5 GHz 5G Urban Macrocells

Muhammad Yaser*

Electrical Engineering, Universitas Pancasila Jakarta

*Corresponding Author, email: muhammadyaser@univpancasila.ac.id

Abstract

Inter-cell interference is still a major bottleneck in 3.5 GHz 5G urban macrocells, and it hits cell-edge users the hardest, leading to low SINR and unequal user throughput. This work studies a two-layer fractional frequency reuse (FFR) scheme that divides a macrocell into inner and outer regions using a fixed threshold radius, then splits a 100 MHz carrier into two separate subbands for the two regions. Performance is evaluated through Monte Carlo simulations using a 3D UMa path-loss model, realistic macro base-station EIRP, and a first-tier interference setting, where the outer region operates with reuse-3 while the inner region uses a reduced (thinned) reuse pattern. Four bandwidth splits between inner and outer regions are tested (25/25, 30/20, 20/30, and 15/35 MHz), and the comparison focuses on total cell capacity, spectral efficiency, and Jain's fairness index. The results show a clear trade-off: giving more bandwidth to the inner region delivers the highest throughput, with the 30/20 MHz split producing cell capacity above 310 Mbps and spectral efficiency of 6.2 bit/s/Hz, but also the lowest fairness at 0.66. Shifting bandwidth toward the outer region improves fairness, reaching 0.82 for 20/30 MHz and 0.86 for 15/35 MHz, but reduces capacity to 260 Mbps and 234 Mbps and spectral efficiency to 5.2 bit/s/Hz and 4.7 bit/s/Hz. Overall, the study highlights how bandwidth partitioning should be chosen based on whether the priority is maximizing total throughput or improving fairness for cell-edge users.

Keywords: Fractional Frequency Reuse, Bandwidth partitioning, Inter-cell interference, 5G

1. Introduction

The rapid deployment of fifth-generation (5G) cellular networks in the 3.5 GHz band is driven by the need to support enhanced Mobile Broadband (eMBB) services with high data rates and massive connectivity [1], [2]. Even with advanced link adaptation and interference coordination techniques, edge users typically experience a lower signal-to-interference-plus-noise ratio (SINR) and, consequently, lower throughput compared to users in the cell-center region [3] .This motivates the continued investigation of interference-aware radio resource management schemes that can exploit the spatial structure of the cell and user distribution.

Fractional Frequency Reuse (FFR) is a well-established interference coordination technique that partitions the cell area into inner and outer regions, assigning different reuse patterns to each region [4], [5]. Conventional FFR schemes usually adopt a single-layer structure with a fixed reuse-1 pattern in the inner region and a more conservative reuse (e.g., reuse-3) in the outer region, combined with a pre-defined partition of the carrier bandwidth among reuse subbands [6], [7]. Prior works have shown that such schemes can significantly improve cell-edge performance compared with pure reuse-1. However, they often assume a fixed bandwidth split and focus primarily on user-level SINR or edge

throughput metrics, rather than systematically characterizing the trade-off between total capacity, spectral efficiency, and fairness at the cell level [8], [9]. Moreover, many studies concentrate on single-layer layouts and do not explicitly consider the effect of splitting the carrier into inner and outer "layers" with separate power and bandwidth allocations [10]. In practice, the choice of how much bandwidth to allocate to the inner and outer regions is a non-trivial matter. Allocating a larger fraction of the spectrum to the high-SINR inner region is expected to increase the aggregate cell capacity and spectral efficiency, because more resources are devoted to users with better channel conditions [11], [12], [13]. On the other hand, allocating more bandwidth to the outer region can improve the quality of service for cell-edge users and enhance fairness across the user population, at the cost of some reduction in total throughput. Existing FFR studies typically do not quantify this trade-off in a controlled setting where the FFR geometry, transmit power, and interference model are fixed, and only the inner–outer bandwidth partition is varied [14], [15], [16]. As a result, there is limited guidance on how to select an appropriate bandwidth split for a given deployment objective (throughput-oriented versus fairness-oriented).

Motivated by this gap, this paper investigates a two-layer FFR configuration in which a single macrocell is divided into inner and outer regions by a fixed threshold radius, and the carrier is split into two disjoint subbands assigned to the inner and outer layers, respectively. Under a realistic 3.5 GHz macrocell setting with a 100 MHz carrier, realistic macro-BS EIRP levels, and an interference model based on a first-tier ring of neighboring cells, we numerically evaluate the impact of different inner–outer bandwidth partitions on key performance indicators. Specifically, four bandwidth splits are considered (25/25, 20/30, 30/20, and 15/35 MHz for inner/outer), and their effect on total cell capacity, cell spectral efficiency, and Jain's Fairness Index is analyzed.

The main contributions of this work are threefold. First, we develop a simulation framework for two-layer FFR in a macrocell scenario that combines a 3D UMa path-loss model, realistic BS transmit powers, and an explicit interference model with different reuse patterns for the inner and outer layers. Second, we provide a systematic performance comparison of multiple inner–outer bandwidth partitions, highlighting how shifting bandwidth toward the inner or outer region influences the distributions of cell capacity and the resulting spectral efficiency. Third, we quantify the trade-off between throughput efficiency and fairness using Jain's Fairness Index, showing that configurations that favor the inner layer maximize cell capacity and spectral efficiency, whereas configurations that favor the outer layer improve fairness among users. These insights can serve as practical guidelines for selecting bandwidth partitions in two-layer FFR deployments, depending on whether the operator prioritizes aggregate throughput or fairness of service.

The rest of this paper is structured as follows: Section II outlines the two-layer FFR system model, Section III details the simulation methodology and discusses the numerical results, and Section IV concludes the work.

2. System Model

This section describes the two-layer FFR system model and the numerical simulation framework used in the performance evaluation. The main channel, power, and configuration parameters are summarized separately in Table 1.

2.1 Network layout and FFR configuration

We consider a single macrocell with a base station (BS) located at the cell center. The cell area is partitioned into two regions, namely an inner region and an outer region, using a fixed threshold radius R_{th}. A two-layer FFR scheme is adopted by splitting the carrier into two disjoint subbands dedicated to the inner and outer layers, respectively. Several inner–outer bandwidth partitions are investigated to study the trade-off between concentrating spectrum in the cell-center region and in the cell-edge region.

The inner layer operates with a more aggressive reuse (close to reuse-1), whereas the outer layer employs a more conservative reuse pattern to protect cell-edge users from inter-cell interference. The BS transmit powers in the inner and outer layers are modeled with realistic EIRP levels, with the outer layer generally having a higher EIRP than the inner layer.

2.2 User Distribution

In each simulation drop, users are randomly placed within the cell according to a prescribed composition between inner and outer users (e.g., a balanced inner–outer scenario). User positions are generated according to an area-uniform distribution, where both the radial distance and azimuth angle are randomized such that the user density is uniform over the cell area. The resulting Cartesian coordinates are then used to compute the three-dimensional distances to the serving BS and to the neighboring BSs that act as interferers.

2.3 Channel, noise, and interference models

The downlink path loss is modeled using a three-dimensional Urban Macro (UMa) model that depends on the 3D distance and the carrier frequency. From the path-loss values, large-scale channel gains are obtained for both the serving and interfering links. Thermal noise is modeled through its power spectral density $N_0 = kTF$, where $k$is Boltzmann's constant, T is the noise temperature, and $F$is the receiver noise factor corresponding to the UE noise figure. For the inner and outer bandwidths B_{in} and B_{out}, the total noise powers are

$$N_{\text{in}} = N_0 B_{\text{in}}, \qquad N_{\text{out}} = N_0 B_{\text{out}}. \tag{1}$$

Inter-cell interference is modeled using a first-tier ring of neighboring BSs arranged on a hexagonal lattice. For the outer layer, a reuse-3 pattern is assumed, so that only a subset of neighboring BSs is co-channel with the serving BS. For the inner layer, a thinned reuse pattern is applied, where only a subset of neighbors contributes co-channel interference, representing a light inter-cell interference coordination (ICIC) regime.

2.4 SINR, capacity, and performance metrics

The downlink SINR of an inner-region user is defined as

$$\gamma_{\text{in}} = \frac{P_{\text{t,in}} G_{\text{in}}}{I_{\text{in}} + N_{\text{in}}} \tag{2}$$

where $P_{\text{t,in}}$ is the inner-layer transmit power, G_{in} is the serving-link channel gain, I_{in} is the aggregate co-channel interference from neighboring BSs, and N_{in} is the noise power in the inner subband.

Similarly, the SINR for an outer-region user is given by

$$\gamma_{\text{out}} = \frac{P_{\text{t,out}} G_{\text{out}}}{I_{\text{out}} + N_{\text{out}}} \tag{3}$$

With analogous notation for the outer layer.
Each layer shares its bandwidth equally among the users it serves. The instantaneous throughput of an inner user and an outer user is expressed as

$$C_{u,\text{in}} = \frac{B_{\text{in}}}{N_{\text{in}}} \log_2(1 + \gamma_{in}) \tag{4}$$

$$C_{u,\text{out}} = \frac{B_{\text{out}}}{N_{\text{out}}} \log_2(1 + \gamma_{out})$$

where $N_{\text{in}}$and N_{out} denote the numbers of users in the inner and outer regions, respectively. The total cell capacity is then defined as

$$C_{\text{cell}} = \sum_{u \in \text{inner}} C_{u,\text{in}} + \sum_{u \in \text{outer}} C_{u,\text{out}} \tag{5}$$

and the cell spectral efficiency is given by

$$\eta_{\text{cell}} = \frac{C_{\text{cell}}}{B_{\text{in}} + B_{\text{out}}} \tag{6}$$

The fairness of the throughput distribution across users is quantified by Jain's Fairness Index:

$$J = \frac{(\sum_u C_u)^2}{N_{\text{UE}} \sum_u C_u^2} \tag{7}$$

where C_u is the throughput of user u and N_{UE} is the total number of users in the cell.

The performance of each bandwidth-allocation configuration is evaluated using a Monte Carlo simulation with a large number of independent trials. In each drop, user positions are regenerated, the channel and interference are recomputed, and the resulting cell capacity, spectral efficiency, and fairness index are obtained. From these realizations, empirical distributions, mean values, and statistical confidence intervals are derived to assess the impact of inner–outer bandwidth partitioning on capacity, spectral efficiency, and fairness in the considered two-layer FFR system.

3. Results and discussion

Section 3 presents the numerical results for the proposed two-layer FFR scheme based on Monte Carlo simulations under the system model described in Section 2. The evaluation assumes a single macrocell operating in the 3.5 GHz band with a 100 MHz carrier, realistic macro-BS EIRP levels for the inner and outer layers, and a UE receiver noise figure of 7 dB. A fixed threshold radius is used to separate inner and outer regions, and a balanced traffic scenario with 50 inner and 50 outer users per cell is considered. Inter-cell interference is modeled through a first-tier ring of six neighboring sites, with a reuse-3 pattern for the outer layer and a thinned reuse pattern for the inner layer.

Table 1. Simulation Parameters

Parameter	Values
Cell Radius	2000 m
Boundary radius inner outer	1000m
BS height	25 m
UE height	1.75 m
Inner center frequency	3.4125 GHz
Outer center frequency	3.4875 GHz
Outer BS transmit power	53 dBm
Outer BS transmit power	50 dBm
Total carrier bandwidth	100 MHz

The main simulation parameters are summarized in Table 1, followed by a detailed discussion of the impact of four inner–outer bandwidth partitions (25/25, 20/30, 30/20, and 15/35 MHz) on key performance indicators, namely cell capacity, cell spectral efficiency, and Jain's Fairness Index, as depicted in Figures 1–4

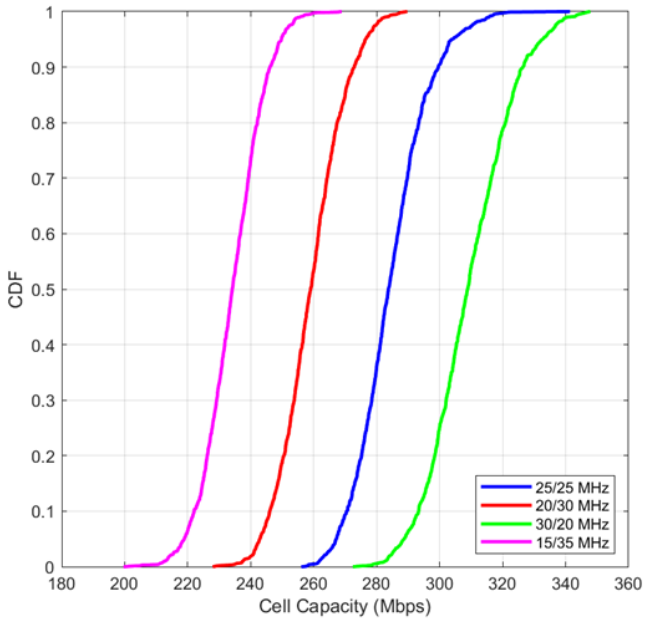

Figure 1. CDF of cell capacity under different inner–outer bandwidth partitions

Figure 1 depicts the CDF of total cell capacity for four inner–outer bandwidth partitions, namely 25/25, 20/30, 30/20, and 15/35 MHz, under otherwise identical system settings. A clear horizontal separation is observed among the curves, indicating that the bandwidth split has a substantial impact on the achievable cell throughput distribution. The configuration that allocates a larger portion of the spectrum to the inner region (30/20 MHz) consistently yields the highest capacities: its median cell capacity is around 309 Mbps, and even at the 10th percentile, the capacity remains above approximately 290 Mbps. The symmetric 25/25 MHz baseline performs slightly worse, with the CDF shifted left by about 20–30 Mbps across most probability levels. When more bandwidth is shifted toward the outer region, the entire CDF moves further to the left, indicating a systematic degradation in total cell capacity. The 20/30 MHz split reduces the median capacity to roughly 260 Mbps. In contrast, the most outer-favored configuration,

15/35 MHz (magenta curve), exhibits the lowest performance, with median capacity near 230 Mbps and the upper tail limited to below about 260 Mbps. The slopes of all four curves remain relatively similar, suggesting that the main effect of changing the bandwidth partition is a change in the mean level rather than in the variability of cell capacity. Overall, these results confirm that, for the considered scenario, assigning a larger fraction of spectrum to the high-SINR inner region significantly improves aggregate cell throughput, whereas aggressively prioritizing spectrum for the outer region leads to a noticeable reduction in total cell capacity.

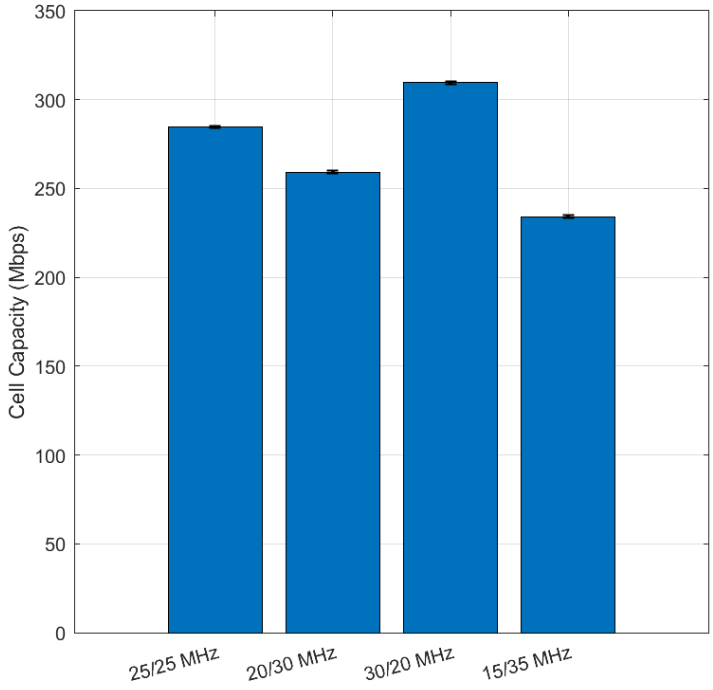

Figure 2. Average cell capacity for different inner–outer bandwidth partitions.

Figure 2 reports the average cell capacity for four inner–outer bandwidth partitions, namely 25/25, 20/30, 30/20, and 15/35 MHz, with error bars indicating the variation across Monte Carlo realizations. The 30/20 MHz configuration achieves the highest average cell capacity, slightly above 310 Mbps, showing that allocating a larger portion of spectrum to the inner region where channel conditions are generally better can maximize the aggregate cell throughput. The symmetric 25/25 MHz split comes second at around 285 Mbps, while the more outer-oriented 20/30 MHz scheme reduces the average capacity to roughly 260 Mbps. The most outer-dominant allocation, 15/35 MHz, yields the lowest cell capacity, only about 234 Mbps. The error bars for all four bars are relatively small compared with their mean values, indicating that the observed differences in capacity are not due to random fluctuations but represent a consistent effect of the different bandwidth partitions. Overall, these results confirm that, for the two-layer FFR configuration considered, an overly aggressive shift of spectrum towards the outer layer degrades the total cell capacity, whereas assigning a larger bandwidth share to the inner layer provides a clear throughput gain at the cell level.

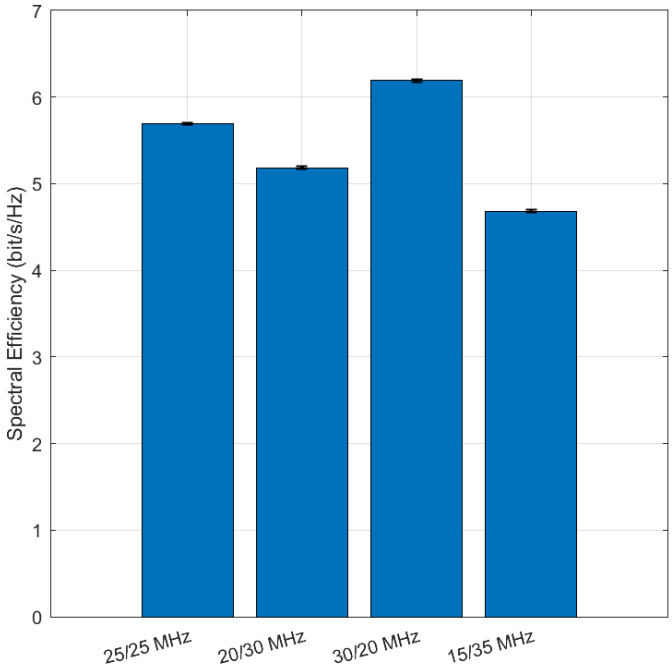

Figure 3. Average Cell Spectral Efficiency for Different Inner–Outer Bandwidth Partitions.

Figure 3 shows the average cell spectral efficiency for four inner–outer bandwidth partitions, namely 25/25, 20/30, 30/20, and 15/35 MHz, with error bars representing the variation across simulation runs. The 30/20 MHz configuration achieves the highest spectral efficiency, slightly 6.2 bit/s/Hz, indicating that assigning a larger fraction of bandwidth to the inner region where channel conditions are generally better allows more effective use of each Hertz of spectrum. The symmetric 25/25 MHz split ranks second at about 5.7 bit/s/Hz, followed by the 20/30 MHz scheme at around 5.2 bit/s/Hz. In contrast, the most outer-oriented allocation, 15/35 MHz, yields the lowest spectral efficiency, only about 4.7 bit/s/Hz. The relatively small error bars for all four bars suggest that these differences are consistent and not merely due to statistical fluctuations. Overall, the results indicate that, for the two-layer FFR configuration considered, shifting too much bandwidth to the outer layer degrades cell-level spectral efficiency, whereas giving a larger share of bandwidth to the inner layer provides a clear efficiency gain.

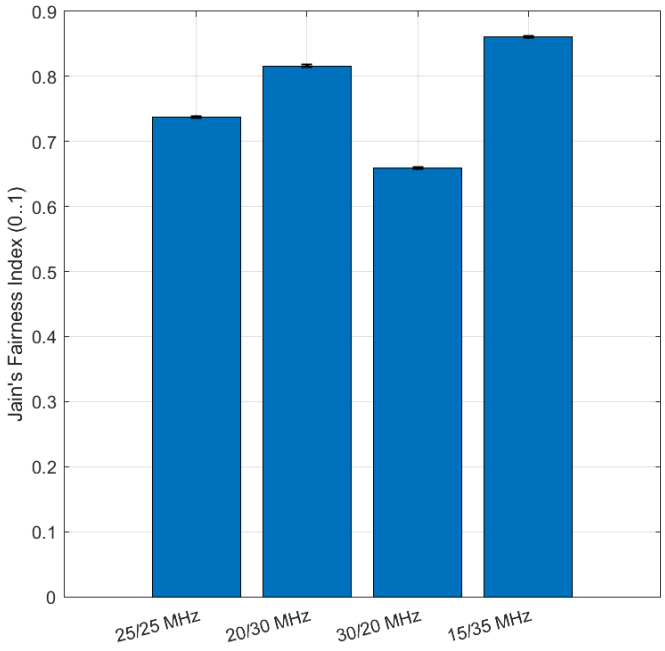

Figure 4. Average Jain's Fairness Index for Different Inner–Outer Bandwidth Partitions.

Figure 4 reports the average value of Jain's Fairness Index for four inner–outer bandwidth partitioning schemes, namely 25/25, 20/30, 30/20, and 15/35 MHz, together with error bars that illustrate the variability across simulation realizations. The configuration that most favors the outer layer, i.e., 15/35 MHz, yields the highest fairness, with an index close to 0.87. The 20/30 MHz scheme follows with a value of around 0.82, whereas the symmetric 25/25 MHz configuration attains about 0.74. In contrast, the 30/20 MHz split, which prioritizes the inner layer, achieves the lowest fairness, with an index of only about 0.66. This pattern indicates that allocating a larger portion of the spectrum to the outer region which is typically populated by cell-edge users with poorer channel conditions can enhance the uniformity of throughput among users. The relatively small error bars for all bars suggest that the differences in fairness across the four scenarios are stable and not merely due to statistical fluctuations. Overall, these results confirm the presence of a trade-off between capacity efficiency and service fairness: configurations that strongly favor the inner layer (such as 30/20 MHz) tend to increase the average cell throughput but at the cost of reduced fairness, whereas more generous bandwidth allocations to the outer layer (20/30 and 15/35 MHz) improve the fairness of throughput distribution across users.

4. Conclusion

This paper looks at how a two-layer FFR scheme performs in a 3.5 GHz macrocell, where the cell is split into inner and outer regions, and the bandwidth is divided between them using four options: 25/25, 20/30, 30/20, and 15/35 MHz. The results clearly show a trade-off between throughput and fairness. When more bandwidth is given to the inner region (30/20 MHz), the system delivers the highest average cell capacity just above 310 Mbps and the best spectral efficiency, around 6.2 bit/s/Hz, but at the cost of fairness, with Jain's index dropping to about 0.66. On the other hand, when more bandwidth is shifted to the outer region, especially with the 20/30 MHz and 15/35 MHz splits, fairness improves (Jain's index rises to roughly 0.82 and 0.87, respectively), but both capacity and spectral efficiency decline, the average capacity falls to about 260 Mbps and 234 Mbps,

and spectral efficiency to around 5.2 and 4.7 bit/s/Hz. In practice, this means that the best bandwidth split in a two-layer FFR system depends on what the operator cares about more: maximizing total throughput or ensuring fairer service for cell-edge users.

Acknowledgements

We thank all those who willing to help us in completing this research and the editorial team of Jurnal Teknik Elektro Indonesia who has published this paper.

References

[1] M. I. Rochman *et al.*, "A comprehensive analysis of the coverage and performance of 4G and 5G deployments," *Computer Networks*, vol. 237, p. 110060, Dec. 2023, doi: 10.1016/j.comnet.2023.110060.

[2] E. Björnson, F. Kara, N. Kolomvakis, A. Kosasih, P. Ramezani, and M. B. Salman, "Enabling 6G Performance in the Upper Mid-Band by Transitioning From Massive to Gigantic MIMO," 2024, *arXiv*. doi: 10.48550/ARXIV.2407.05630.

[3] K. Bechta, C. Ziółkowski, J. M. Kelner, and L. Nowosielski, "Modeling ofDownlinkInterference in Massive MIMO 5G Macro-Cell," *Sensors*, vol. 21, no. 2, p. 597, Jan. 2021, doi: 10.3390/s21020597.

[4] T. D. Novlan, R. K. Ganti, A. Ghosh, and J. G. Andrews, "Analytical Evaluation of Fractional Frequency Reuse for Heterogeneous Cellular Networks," *IEEE Trans. Commun.*, vol. 60, no. 7, pp. 2029–2039, Jul. 2012, doi: 10.1109/TCOMM.2012.061112.110477.

[5] M. Seo, S.-H. Chang, J.-M. Lee, K.-H. Kim, H. Park, and S.-H. Kim, "Optimal Coverage of Full Frequency Reuse in FFR Networks in Relation to Power Scaling of a Base Station," *Sensors*, vol. 23, no. 21, p. 8925, Nov. 2023, doi: 10.3390/s23218925.

[6] S. C. Lam and X. N. Tran, "Fractional Frequency Reuse in Ultra Dense Networks," *Physical Communication*, vol. 48, p. 101433, Oct. 2021, doi: 10.1016/j.phycom.2021.101433.

[7] D. Lin, "Comparison of FFR+IFR and IFR Models with Different Frequency Reuse Factors in Cellular Networks," *HSET*, vol. 27, pp. 575–579, Dec. 2022, doi: 10.54097/hset.v27i.3818.

[8] M. Rahman and H. Yanikomeroglu, "Enhancing cell-edge performance: a downlink dynamic interference avoidance scheme with inter-cell coordination," *IEEE Trans. Wireless Commun.*, vol. 9, no. 4, pp. 1414–1425, Apr. 2010, doi: 10.1109/TWC.2010.04.090256.

[9] X. Zhang *et al.*, "Cell Edge User Capacity-Coverage Reliability Tradeoff for 5G-R Systems With Overlapped Linear Coverage," *IEEE Trans. Intell. Transport. Syst.*, vol. 23, no. 10, pp. 17936–17951, Oct. 2022, doi: 10.1109/TITS.2022.3174671.

[10] X. Han *et al.*, "Flexible Spectrum Orchestration of Carrier Aggregation for 5G-Advanced," 2023, doi: 10.48550/ARXIV.2305.15890.

[11] T. D. Novlan, R. K. Ganti, A. Ghosh, and J. G. Andrews, "Analytical Evaluation of Fractional Frequency Reuse for OFDMA Cellular Networks," *IEEE Trans. Wireless Commun.*, vol. 10, no. 12, pp. 4294–4305, Dec. 2011, doi: 10.1109/TWC.2011.100611.110181.

[12] R. Y. Chang, Z. Tao, J. Zhang, and C.-C. Kuo, "A Graph Approach to Dynamic Fractional Frequency Reuse (FFR) in Multi-Cell OFDMA Networks," in *2009 IEEE International Conference on Communications*, Dresden, Germany: IEEE, Jun. 2009, pp. 1–6. doi: 10.1109/ICC.2009.5198612.

[13] D. Tse and P. Viswanath, *Fundamentals of Wireless Communication*, 1st ed. Cambridge University Press, 2005. doi: 10.1017/CBO9780511807213.

[14] S.-H. Chang, H.-G. Park, S.-H. Kim, and J. P. Choi, "Study on Coverage of Full Frequency Reuse in FFR Systems Based on Outage Probability," *IEEE Trans. Commun.*, vol. 66,

no. 11, pp. 5828–5843, Nov. 2018, doi: 10.1109/TCOMM.2018.2859326.

[15] N. U. Hassan and M. Assaad, "Optimal Fractional Frequency Reuse (FFR) and resource allocation in multiuser OFDMA system," in *2009 International Conference on Information and Communication Technologies*, Karachi, Pakistan: IEEE, Aug. 2009, pp. 88–92. doi: 10.1109/ICICT.2009.5267207.

[16] R. Y. Chang, Z. Tao, J. Zhang, and C.-C. Kuo, "A Graph Approach to Dynamic Fractional Frequency Reuse (FFR) in Multi-Cell OFDMA Networks," in *2009 IEEE International Conference on Communications*, Dresden, Germany: IEEE, Jun. 2009, pp. 1–6. doi: 10.1109/ICC.2009.5198612.